Inorganica Chimica Acta, 21 (1977) 65–74

Photoaction In the Course of Chelate Formation III. Ligand Spin-Reversal Enhancements by Heavy-Metal Ions and Their Influences on the Excited-State ^{3}(Borobenzoylacetonide) Complex Formation

M. MARCANTONATOS

Department of Inorganic and Analytical Chemistry, University of Geneva, Geneva, Switzerland

Received June 4, 1976

The 1/1 "borobenzoylacetonide" chelate formation, in 8% (V/V) H_2SO_4/EtOEt solvent, has been investigated in the presence of Ag^+, Cd^{2+}, Hg^{2+}, Tl^+, under continuous ligand excitation at its ICT band. It is shown that the above metal ions (M^{n+}) affect both ground-state and excited-state (T_1) interactions of benzoylacetone (BZA) with boron species. Ground-state influences are found to be attributable to BZA EDA complexes with M^{n+} formed most probably by the two-way actions: $\pi_{2(benzene\,ring)}$ or π_3 to s A.O. (Ag^+, Cd^{2+}, Hg^{2+}) and to 6pA.O. (Tl^+) and $d\pi_y$ A.O. to $\pi^*_{2(benzene\,ring)}$ electron donation.

$T \longleftrightarrow S$ crossings of the BZA's conjugate chelate form are found to be enhanced by all the above metal ions. Influences of these enhancements, on the ^{3}BZA interaction with boron species, are quantitatively analysed.

Introduction

Since it has recently been shown [1] that enhancement of spin-reversal processes of benzoylacetone (BZA) by the heavy-atom molecule C_2H_5I affects the rate of its lowest triplet state complexation by boron species, our interest was centered on the influence of heavy-metal ions on this excited-state complexation.

General effects of inorganic molecules [3–5], anions [6–9], metal ions [10–15], metal complexes [16–21] and organometallics [22–24] on an organic compound, are quenchings of its lowest excited states by a number of mechanisms depending on the electronic structure and spectroscopic properties of both organic compound and perturber.

Electronic energy transfer to, assisted (heavy-atom) spin-reversal* by, or electron transfer to, or from, the perturbing species, are the most common routes for depleting the lowest excited states of an organic molecule, while direct population of its lowest triplet may be considerably assisted by "organic compound–inorganic or organic compound–organometal complex" CT states [17, 18, 24].

When undertaking the present investigation on possible effects of some heavy-metal ions in the complexation of boron species by ^{3}BZA [1, 2], the following starting assumptions were made:

a) Heavy-metal ions (HMI) are expected to enhance $T \longleftrightarrow S$ processes of BZA and therefore modify the ^{3}(borobenzoylacetonide) yield.

(b) HMI with relatively pronounced oxidative tendencies are also expected to produce analogous modifications by ^{1} or ^{3}BZA-to-metal ion electron transfer and therefore more active $T \longleftrightarrow S$ crossings of the loose ^{1} or ^{3}EDA complexes.

c) Possible ground-state BZA-to-metal ion coordination or even weak EDA interaction, are expected to result in ^{1}BZA static quenching and therefore to decrease the yields of ^{3}BZA and ^{3}(B-BZA) complexes.

d) Possible ^{1} or ^{3}BZA energy transfer to metal ion is also expected to result in a decrease of the above triplet yields, while the presence in the metal ions of unpaired electrons is expected to favour the ^{1} or ^{3}BZA crossings.

In order to avoid possible paramagnetic effects and electronic energy transfer, the present investigation of the borobenzoylacetonide 1/1 chelate formation under ligand excitation [1, 2] was carried out in the presence of Ag^+, Cd^{2+}, Hg^{2+} and Tl^+.

To our knowledge, effects of foreign metal ions on photo-induced or photo-assisted complexations have not as yet been investigated. In the present paper, we report and discuss results of such an investigation.

Experimental

Reagents were purified and solutions prepared as described in part I of this work [2]. Ether was of "Uvasol" quality Merck. Metal ion solutions in SE

*It may appear not to be necessary to dissociate this mechanism from the CT (electron transfer) one. However, since indirect S, T mixing via perturbed–perturber CT states does not seem to be the unique $S \longleftrightarrow T$ enhancing route and since no heavy-atom perturbers also assist $S \longleftrightarrow T$ crossings [25, 26], we may maintain this distinction.

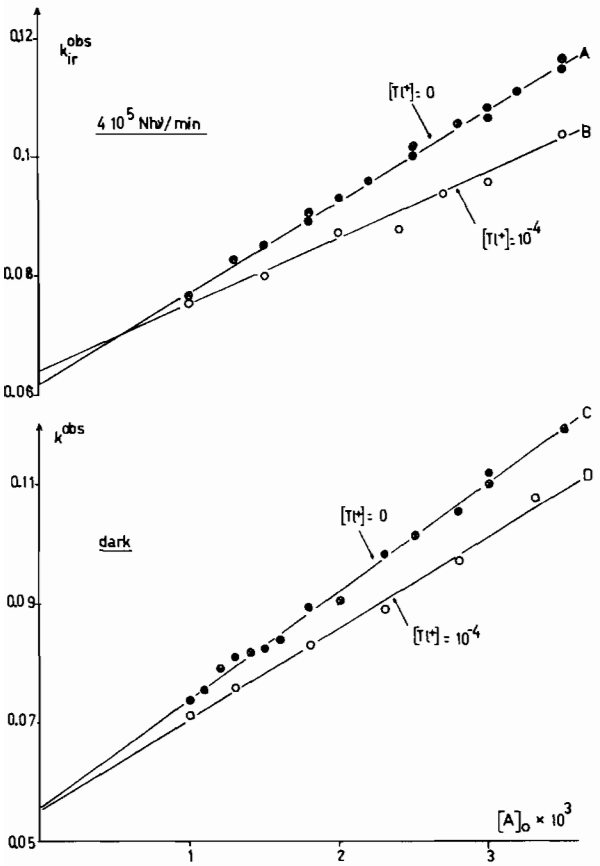

Fig. 1. Observed rate constants of the 1/1 borobenzoylacetonide chelate formation, without irradiation (D and C) and under continous ligand excitation (B and A) in the presence of Tl^+: ○–, of NO_3K (10^{-4} M) ●– and without Tl^+ ⊕– (A and C). BZA = 10^{-5}.

solvent (sulfuric (96%) acid/EtOEt (8% V/V)) were always prepared from fresh sulfuric solutions (containing 2.5% H_2O (V/V)) of Ag^+ and Tl^+ (5×10^{-3}), Cd^{2+} and Hg^{2+} (5×10^{-4}).

$AgNO_3$, $TlNO_3$, $3CdSO_4 \cdot 8H_2O$ and $HgSO_4$ were of *"pro analysi"* quality Merck.

Irradiations ($I'_0 = 4 \times 10^{-5}$ Nhν/min) of solutions at 20 °C were performed under the same conditions as previously [2], in an apparatus assembly described in part I [2] of this work.

Results and Discussion

Ground and Excited Ligand Interaction with Boron Species in the Presence of Heavy-metal Ions (HMI)

As shown in parts I [2] and II [1], the relevant rate parameters for the chelate formation under continuous ligand excitation at its ICT band (310 nm) are*:

*For notations see parts I and II.

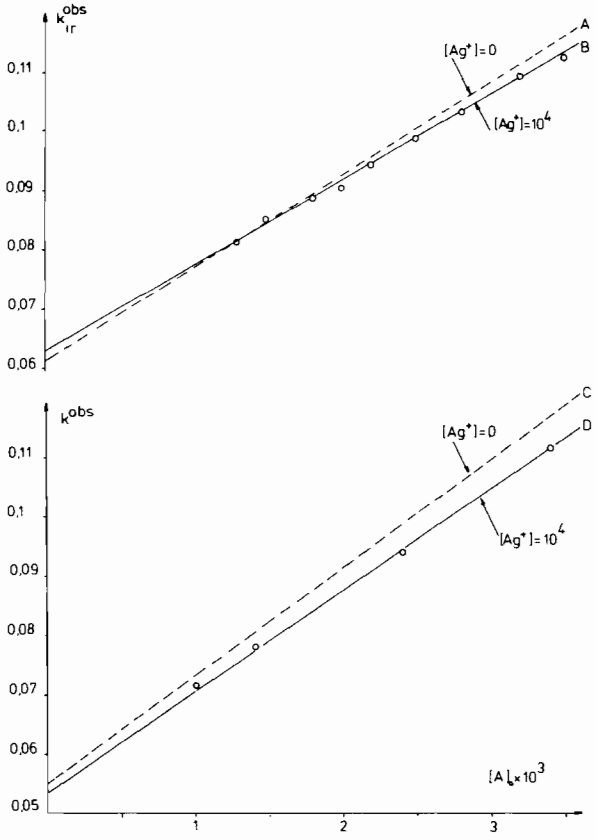

Fig. 2. *(For caption see opposite.)*

$$\overleftarrow{k}_{ir} = \frac{k_{34}\Phi_{ST}\epsilon_R V^{-1} GI'_0}{k'_{32} + k_{34}} + \frac{k'_{32}k'_{43}}{k'_{32} + k_{34}} = M + W \quad (1)$$

$$\overrightarrow{k}_{ir} = \frac{k_{34}k_{23}k_1 k_{-1}^{-1} k_{12}[H^+]}{(k'_{32} + k_{34})(k_{21} - \phi^{**}\epsilon_{RH}V^{-1}GI'_0)} = N \quad (2)$$

$$k_{ir}^{obs} = [(M + N[A]_0)[R]_0 - U][X]_e^{-1}, \quad (3)$$

$$U = ({}^3k[{}^3R] + {}^3k'[{}^3RH])/(k'_{32} + k_{34}) \quad (3a)$$

Moreover, it could be shown [1, 2] that the above expressions are informative of ligand $S_1 \rightsquigarrow T$ (eq. (1)) and $T_1 \rightarrow S_0$ (eq. (3)) crossings and ligand, other than $S_1 \rightsquigarrow T$, degradations and reversible interactions with solvated proton (eq. (2)).

As can be noticed from the comparison of A and B graphical representations of k_{ir}^{obs} *vs.* $[A]_0$ in Figures 1 to 4, $\overleftarrow{k}_{ir}$ are higher and $\overrightarrow{k}_{ir}$ lower in the presence of HMI but as $\overrightarrow{k}_{ir}$ and $\overleftarrow{k}_{ir}$ are functions of overall forward ($k_{34}\ k_{23}\ k_1\ k_{-1}^{-1}\ k_{12}[H^+]/(k'_{32} + k_{34})k_{21}$) and reverse ($k'_{32}\ k'_{43}/(k'_{32} + k_{34})$) ground-state rate constants, the influence of HMI on dark chelate formation was first investigated.

Ground-state Influences

Surprisingly enough, forward rate constants $\overrightarrow{k}$ of dark chelate formation have lower values (compare

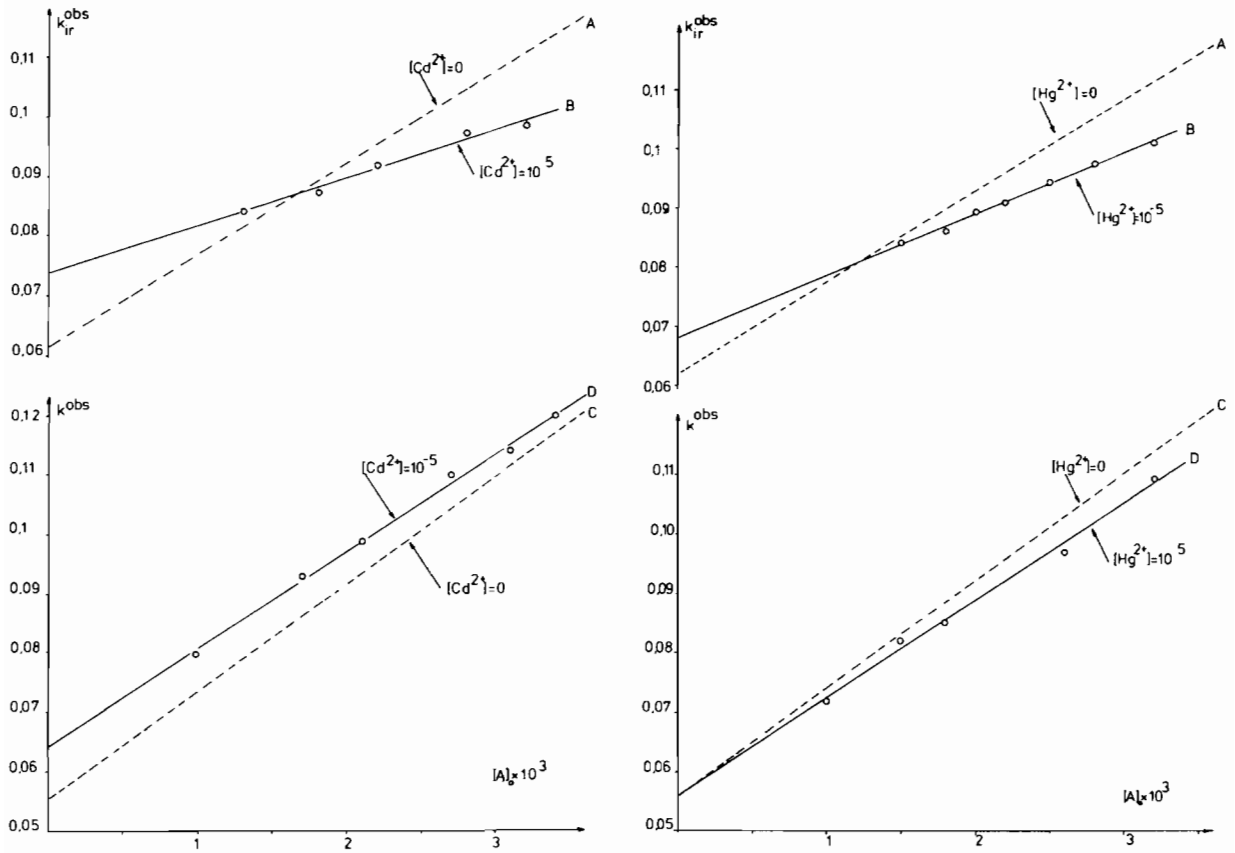

Figs. 3 and 4. Observed rate constants of the 1/1 borobenzoylacetonide chelate formation, without irradiation (D and C) and under continous ligand excitation (B and A). BZA = 10^{-5}.

C and D in Figures 1 to 4) in the presence of HMI, and in the case of Cd^{2+} both $\vec{k}$ and $\overleftarrow{k}$ are affected.

Any possible irreversible BZA interaction with these metal ions can safely be disregarded, since not only all kinetics followed in an absolutely normal manner reversible 1/1 chelate formation (linear regression coefficients for semilogarithmic plots being in all cases higher than 0.999), but also the 310 absorbance of BZA in the presence of HMI did not show any deviation from its initial value, within periods of time largely exceeding the time of boron–BZA chelate equilibrium atteignment. This also excludes the possibility of any catalytic action of HMI on BZA and as will be noticed later on, radiative lifetimes of BZA–HMI species are significantly different.

The remaining most plausible possibility is a non-rate-determining reversible interaction between BZA and metal ion. This can be kinetically justified by the following*:

For Tl^+, Ag^+, Hg^{2+} (M^{n+}):

$$R + B \underset{k'_{-1}}{\overset{k'_1}{\rightleftharpoons}} Y \underset{k'_{-2}}{\overset{k'_2}{\rightleftharpoons}} X \qquad (4)$$

$$R + M^{n+} \overset{\beta_M}{\rightleftharpoons} R\text{–}M^{n+}$$

$$\frac{d[X]}{dt} = \frac{k'_2 k'_1 [A]_0 [R]}{k'_{-1} + k'_2} - \frac{k'_{-1} k'_{-2} [X]}{k'_{-1} + k'_2};$$

$$([B]_0 \gg [R]_0)$$

$$= \frac{k'_2 k'_1 [A]_0([R]_0 - [X])}{(1 + \beta_M [M^{n+}])(k'_{-1} + k'_2)} - \frac{k'_{-1} k'_{-2} [X]}{k'_{-1} + k'_2}$$

$$= \vec{k}(1 + \beta_M [M^{n+}])^{-1} [A]_0([R]_0 - [X]) - \overleftarrow{k}[X]$$

and

$$k^{obs} = \vec{k}_M [A]_0 + \overleftarrow{k} \qquad (5)$$

with

$$\vec{k}_M = \vec{k}(1 + \beta_M [M^{n+}])^{-1} < \vec{k} \qquad (6)$$

where R = BZA, B = boron species*, Y = non chelate

*See also ref. 2.

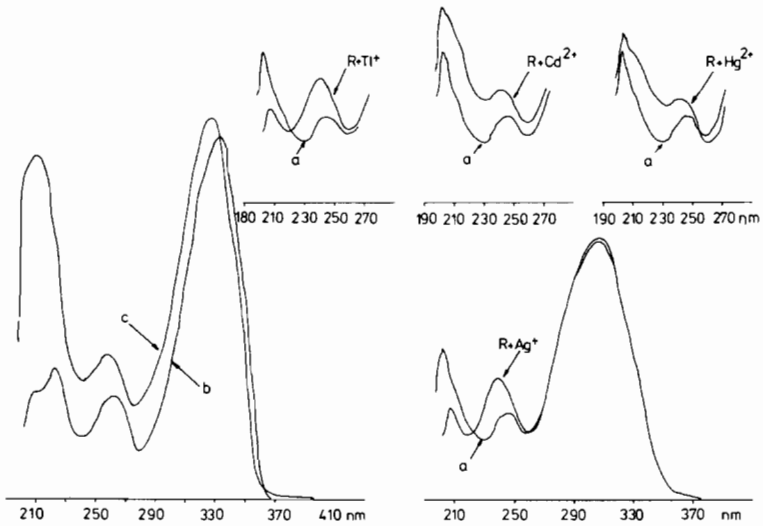

Fig. 5. Absorption spectra of BZA (R): 10^{-5} (a) and BZA (10^{-5}) + metal ion (10^{-4} Ag^+ and Tl^+, 10^{-5} Cd^{2+} and Hg^{2+}). (b) Absorption spectrum of the borobenzoylacetonide chelate ($[BO_3H_3]_0 \gg [BZA]_0$ and these concentrations stand for complete complexation). (c) After addition of 10^{-5} Cd^{2+}.

intermediate, X = chelate, $[A]_0$ = initial boric acid concentration*.

The particular behaviour in the presence of Cd^{2+} can also be kinetically explained by assuming:

$$R + B \underset{k'_{-1}}{\overset{k'_1}{\rightleftharpoons}} Y \underset{k'_{-2}}{\overset{k'_2}{\rightleftharpoons}} X \qquad \beta'_M, M^{n+} \qquad (7)$$

$$k'_{-3} \text{—} X\text{–}M^{n+}$$

so that:

$$\frac{d[X]}{dt} = \frac{k'_2 k'_1 [A]_0([R]_0 - [X])}{(1 + \beta_M[M^{n+}])(k'_{-1} + k'_2)} -$$

$$- \frac{k'_{-1}(k'_{-2} + k'_{-3}\beta'_M[M^{n+}])[X]}{k'_{-1} + k'_2}$$

$$= \vec{k}_M [A]_0([R]_0 - [X]) - \overleftarrow{k}_M [X]$$

and

$$k^{obs} = \vec{k}_M [A]_0 + \overleftarrow{k}_M \qquad (8)$$

with

$$\vec{k}_M = \vec{k}(1 + \beta_M[M^{n+}])^{-1} < \vec{k} \qquad (9)$$

$$\overleftarrow{k}_M = (k'_{-1}k'_{-2} + k'_{-1}k'_{-3}\beta'_M[M^{n+}])/k'_{-1} + k'_{-2} > \overleftarrow{k} \qquad (10)$$

Electronic absorption spectra of BZA in the presence of HMI are shown (Fig. 5) to be distorted in the region of 240 nm*, where metal ion solutions were found to have negligible contributions. As checked by BZA + KNO_3 solutions the counter NO_3^- (in the case of Tl^+ and Ag^+) did not cause any modification in the BZA absorption spectrum, nor had any influence on the kinetics of dark or under irradiation chelate formation (see Fig. 1A and C). However, boron–BZA chelate spectrum shows modifications in the presence of Cd^{2+} and this may account for the $X\text{–}M^{n+}$ interaction assumed in the scheme (7).

As will be seen later, the $BZA\text{–}M^{n+}$ species can be revealed by their 77 °K $S_1 \rightarrow S_0$, $T_1 \rightarrow S_0$ emissions and their radiative lifetimes. They cannot, however, be unambiguously defined, since either EDA complexes or keto–enolate ones seem plausible. Nevertheless, the following observations are in favour of EDA species formation.

First, there is neither hyperchromic, nor red shift in the BZA 310 ICT band, as one would expect if BZA were coordinated to the metal ion in a keto–enolate complex. On the contrary, benzene ring transitions are affected as expected** if electron donation to a A.O. of the metal ion from a low energy bonding benzene M.O. orbital takes effectively place.

Furthermore, $S_1 \rightarrow S_0$ and $T_1 \rightarrow S_0$ emissions of the $BZA\text{–}M^{n+}$ species are vibrationally structured in roughly the same way as BZA, while one would expect, on keto–enolate complex formation, loss or

*See also ref. 2.

*The 205 nm distortion comes from the metal ions, which significantly absorb in this region.

**This point will be discussed in more detail from quantitative data, in a further publication.

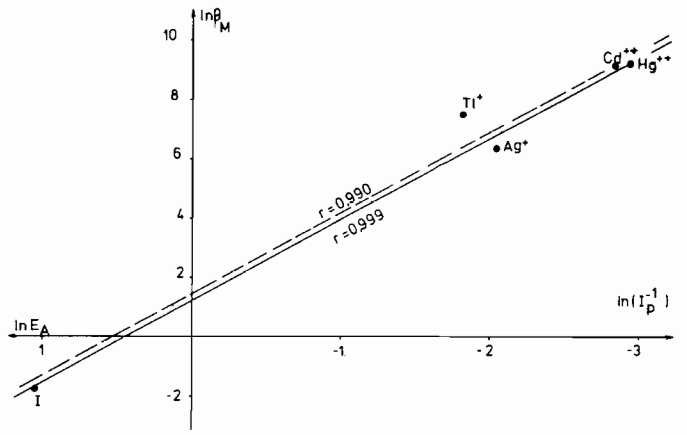

Fig. 6. $\ln\beta_M$ (formation constants of the BZA–M^{n+} species) *vs.* the inverse of ionisation potentials I_p (1st Ag and Tl, 2nd Cd and Hg). E_A electron affinity.

at least blurring of this vibrational structure which is due to the 1,3-enolone cycle of BZA [27].

Moreover, Franck–Condon maxima of the $S_1 \rightarrow S_0$ and $T_1 \rightarrow S_0$ emissions of BZA–M^{n+} are correlated to the inverse of the 1st (for Tl^+, Ag^+) and 2nd (for Cd^{2+}, Hg^{2+}) ionisation potentials (I_p) of the elements as roughly expected for EDA complexes [29, 30].

Finally, calculated values, of β_M by comparison of $\vec{k}$ with $\vec{k}_M$ (see (6)), are also correlated to the inverse of the 1st (for Tl^+, Ag^+) and 2nd (for Cd^{2+}, Hg^{2+}) ionisation potentials of the elements and, interestingly enough, this correlation extends to the electron affinity of iodine for $\beta_{C_2H_5I}$ * calculated from data in part II of this work (Fig. 6).

Figure 6 shows a positive β_M deviation for Tl^+ and a better correlation (r = 0.999) without the Tl^+ point, but it may be argued that this is insignificant for such rough correlations. Nevertheless as will be shown in part IV** of this work, striking deviations from mechanistic correlations for BZA S ⟷ T crossings occur for Tl^+.

It must be pointed out that although for the other metal ions used in this work the accepting orbital is an *s* A.O., in the case of Tl^+ it is the 6*p* A.O. which, owing undoubtedly to its larger expansion, matches better one of the weakly bonding (π_2 or π_3) [31] M.O. of benzene.

From Herman and Skillman [32] calculations, radii of maximum densities are: Ag 4*d*: 0.99 a.u., 5*s*: 2.56; Cd 4*d* 0.95, 5*s* 2.39; Hg 5*d*: 1.13, 6*s*: 2.46; Tl 5*d*: 1.07, 6*s*: 2.28, 6*p*: 2.87.

Undoubtedly, the values of β_M for the BZA–M^{n+} species (compare the rather satisfactory analogy of log $\beta_m(Ag^+)$ = 2.78 with the β of the benzene·Ag^+ complex, log β = 1.66 [33]) are suggestive of metal ion "two-way action"*** with $d\pi_y$ A.O. matching the weakly antibonding π_2^* benzene-ring M.O.

Because of the inertness of the filled 6*s* Tl A.O., 6*s*-to-π_1^*† donation may not be possible and as one observes close orders of the Hg and Tl *d* expansions, the departing behaviour of Tl^+ is to be primarily attributed to the accepting 6*p* A.O.

S_1 and T_1 Species of BZA in the Presence of HMI and Excited-state Influences

As shown in Figures 7 and 8, 77K fluorescence emissions† of BZA, from clear solvent matrices, are perturbed in the presence of metal ions. The same happens to occur for phosphorescence emissions (Fig. 9), while $T_1 \rightarrow S_0$ emissions decay non exponentially.

lnP *vs* t curves, where P stands for the photomultiplier response, clearly show two-component [1, 2] emissions (Figs. 10 to 12) and the following analysis:

$$\ln P = \ln(P_1^0 e^{-t/\tau_1} + P_2^0 e^{-t/\tau_2})$$

$$= \ln P_2^0 - \frac{t}{\tau_2}, \text{ for about } t \geqslant 1.5 \text{ to } 3.5 \text{ sec},$$

$$\ln(P - P_2^0 e^{-t/\tau_2}) = \ln P_1^0 - t/\tau_1$$

leads to the values of τ_1 and τ_2.

Normalisation of the $S_1 \rightarrow S_0$ and $T_1 \rightarrow S_0$ emission intensities at the O–O′ bands of BZA (Figs. 7 to 9) give differences which are the emissions of the BZA–M^{n+} species.

*It is noteworthy that $\beta_{C_2H_5I}$ = 0.196 for BZA–C_2H_5I is quite close to the value of = 0.15 for the benzene–I_2 complex [28].

**To be published.

†As already pointed out in part I [2] of this work, room-temperature fluorescence yield of BZA is very low.

†These emissions are in fact total emissions, but for the slit widths and sensitivity of apparatus used, phosphorescences were negligible.

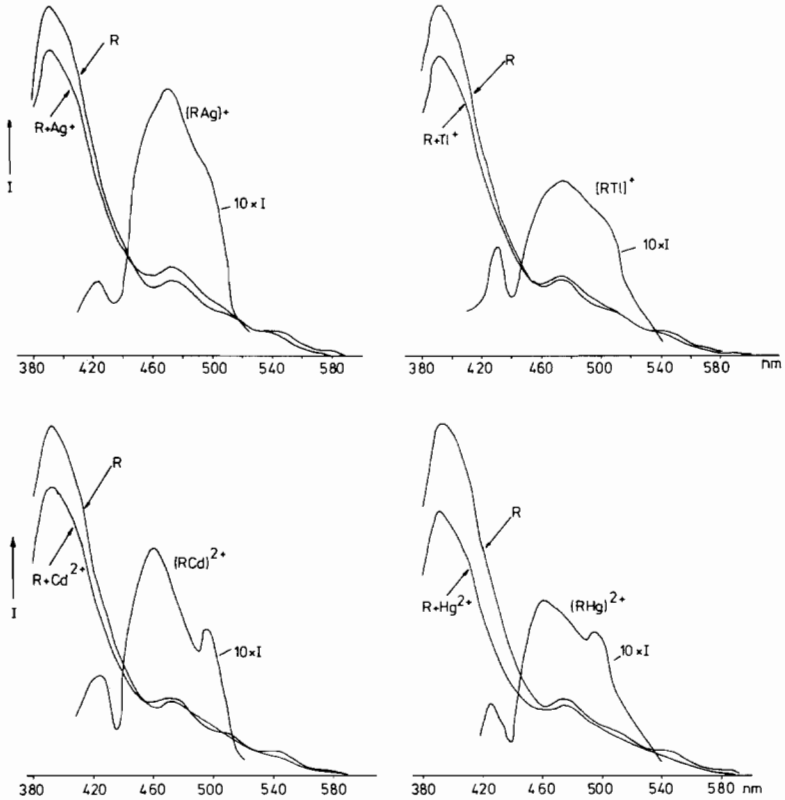

Figs. 7 and 8. 77 K fluorescence spectra from clear solvent matrices of BZA (R): 10^{-3} and of BZA–M^{n+} species (Ag^+, Tl^+: 10^{-4}; Cd^{2+}, Hg^{2+}: 5×10^{-5}). I: photomultiplier response.

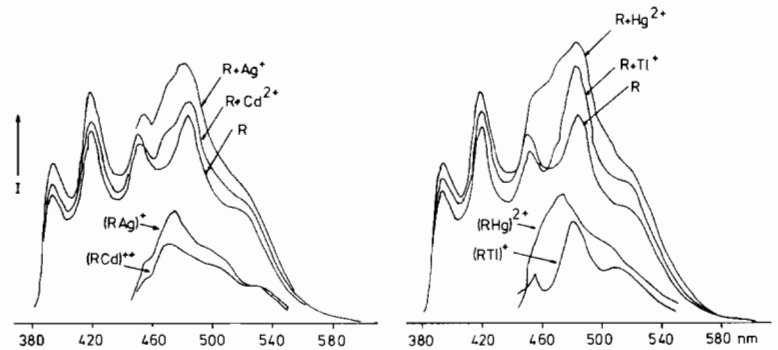

Fig. 9. 77 K phosphorescence spectra from clear solvent matrices of BZA (R): 5×10^{-4} and of BZA–M^{n+} species (Ag^+, Tl^+ 10^{-4}; Cd^{2+}, Hg^{2+}: 5×10^{-5}). I: photomultiplier response.

As frequencies of F–C maxima of these emissions are well correlated to the inverse (I_p^{-1}) of the first ionisation potentials of silver and thallium, and of the second I_p of cadmium and mercury, (Fig. 13) and as there is vibrational structure of the emissions, these spectra, in addition to our other previous arguments, are plausibly attributed to $(BZA–M)^{n+}$ EDA complexes.

Radiative lifetimes τ_1 and τ_2 are then attributed to BZA and $(BZA–M)^{n+}$ and, interestingly enough, τ_1 shortens in the presence of the HMI, as expected for perturbations caused by the HMI.

Noteworthy is also the fact that for $[Ag^+]/[BZA] = 0.02$, $\tau_1 = 1.0$ which is close to the radiative lifetime = 1.2 sec [27] of the imperturbed BZA, but as the $[Ag^+]/[BZA]$ increases to 0.1, τ_1 falls to 0.86 sec.

Now, in order to discuss our kinetic data (Figs. 1 to 4), the combined thermal and photo-excited kinetic scheme for the boron species–BZA interaction given in part I [2] has to be completed, in

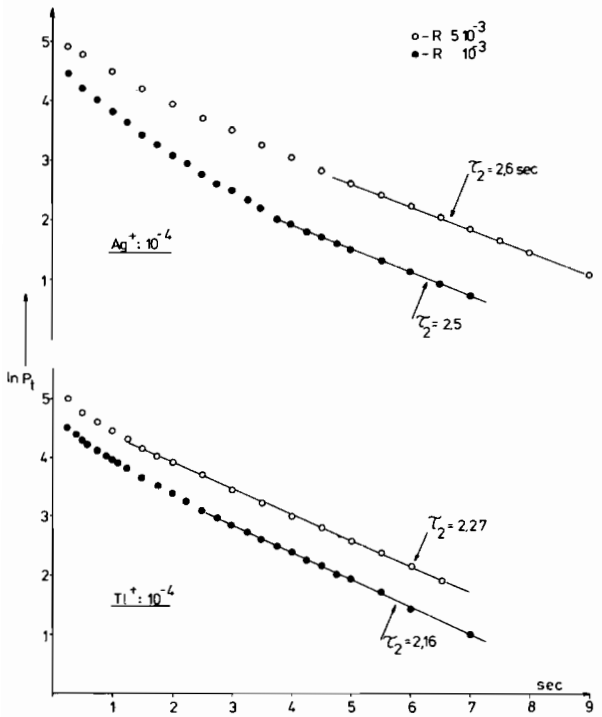

Fig. 10.

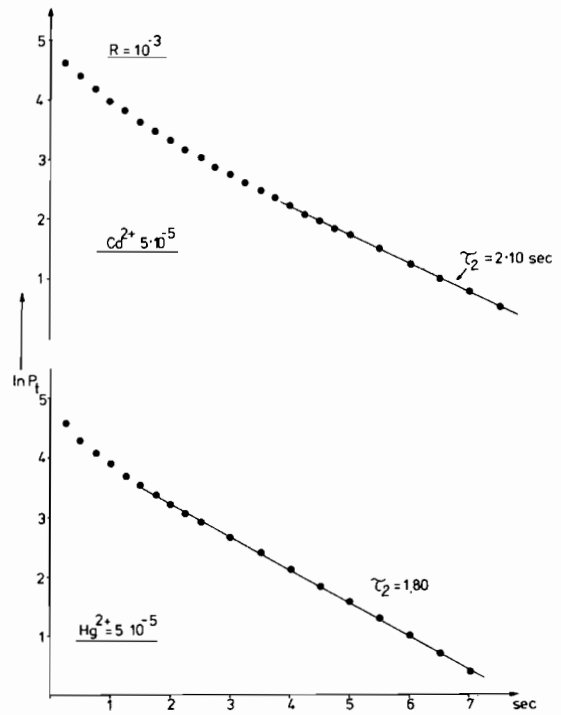

Fig. 11.

the presence of HMI, by:

$$R + M^{n+} \underset{}{\overset{\beta_M}{\rightleftharpoons}} (RM)^{n+} \tag{11}$$

$$(RM)^{n+} \xrightarrow{I_a} {}^1(RM)^{n+} \tag{12}$$

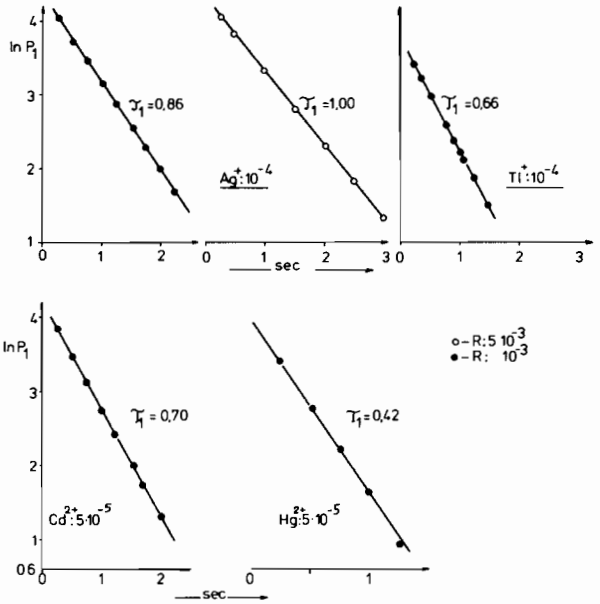

Figs. 10 to 12. Semilogarithmic phosphorescence decay plots for BZA in the presence of Ag^+, Tl^+: 10^{-4}; Cd^{2+}, Hg^{2+}: 5×10^{-5}.

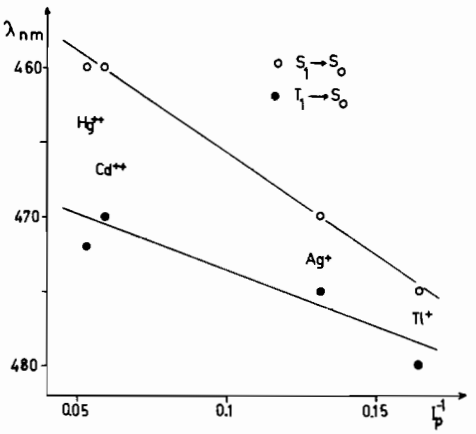

Fig. 13. Wavelengths of Franck–Condon maxima *vs.* inverse of ionisation potentials (1st Ag, Tl; 2nd Cd, Hg).

$$^1(RM)^{n+} \underset{^1k_{-M}}{\overset{\cdot\,^1k_M}{\rightleftharpoons}} {}^1R + M^{n+} \tag{13}$$

$$^1(RM)^{n+} \xrightarrow[k_{C(RM)}]{k_{F(RM)}} (RM)^{n+} \tag{14}$$

$$^1(RM)^{n+} \xrightarrow{k_{ST(RM)}} {}^3(RM)^{n+} \tag{15}$$

$$^3(RM)^{n+} \underset{^3k_{-M}}{\overset{^3k_M}{\rightleftharpoons}} {}^3R + M^{n+} \tag{16}$$

$$^3(RM)^{n+} \xrightarrow[{}^3k_{Q(RM)}[Q]]{k_{TS(RM)}} (RM)^{n+} \qquad (17)$$

An analysis of the B–BZA interaction scheme in the presence of a heavy-atom perturber has been given in part II [1] of this work. This analysis is also applicable to the present case, with the exception that, for the HMI concentrations used (10^{-5} to 10^{-4}), kinetic terms:

$$^{1 \text{ or } 3}k_{-M}[^{1 \text{ or } 3}R][M^{n+}] \qquad (18)$$

are negligible compared to the others.
For example:

$$\frac{d[^1R]}{dt} = I_a - (k_{F(R)} + k_{C(R)} + {}^1k_{Q(R)}[Q] + k_{STM(R)} + {}^1k_{12}[H^+] - {}^1k_{21}[^1RH][^1R]^{-1} + {}^1k_{-M}[M^{n+}] - {}^1k_M[^1(RM)^{n+}][^1R]^{-1})[^1R]$$

$$= I_a - (\sum_i {}^1k_i + k_{STM(R)})[^1R]$$

$$\frac{d[^3R]}{dt} = k_{STM(R)} - (k_{PM(R)} + k_{TSM(R)} + {}^3k_{Q(R)}[Q] + {}^3k_{12}[H^+] - {}^3k_{21}[^3RH][^3R]^{-1} + {}^3k_{-M}[M^{n+}] - {}^3k_M[^3(RM)^{n+}][^3R]^{-1})[^3R]$$

$$= k_{STM(R)} - (\sum_i {}^3k_i + k_{STM(R)} + k_{PM(R)})[^3R]$$

where:

$$\sum_i {}^1k_i = k_{F(R)} + k_{C(R)} + {}^1k_{Q(R)}[Q] + {}^1k_{12}[H^+] - {}^1k_{21}[^1RH][^1R]^{-1} \qquad (19)$$

$$\sum_i {}^3k_i = {}^3k_{Q(R)}[Q] + {}^3k_{12}[H^+] - {}^3k_{21}[^3RH][^3R]^{-1} \qquad (20)$$

$k_{STM(R)}$ and $k_{TSM(R)}$: for $S_1 \rightsquigarrow T$ and $T_1 \rightsquigarrow S_0$ crossings of BZA in the presence of metal ion.

The triplet yield of the conjugate chelate form (R) of BZA* in the presence of HMI, is then given by:

$$\Phi_{STM} = k_{STM}/(\sum_i {}^1k_i + k_{STM}) \qquad (21)$$

and expressions (1), (2) and (3) lead to (see also parts I and II):

$$\overleftarrow{k}_{irM} - \overleftarrow{k}_{GM} = k_{EM} = \frac{k_{34}\Phi_{STM\,R}V^{-1}G_M I'_0}{(k'_{32} + k_{34})(1 + \beta_M[M^{n+}])} \qquad (22)$$

$$\vec{k}_{irM}^{-1} - \vec{k}_{GM}^{-1} = -\phi_M^{**}\epsilon_{RH}V^{-1}G_M I'_0 k_{GM}^{-1}k_{21}^{-1} \qquad (23)$$

$$k_{ir(M)}^{obs} = [(M_M + N_N[A]_0)[R]_0 - U_M]X_e^{-1} \qquad (24)$$

where $\overleftarrow{k}_{GM}$ and $\vec{k}_{GM}$: ground-state reverse and forward overall rate constants for the "B–BZA" chelate formation in the presence of HMI.

$$\vec{k}_{GM} = \vec{k}_G(1 + \beta_M[M^{n+}])^{-1} \qquad (25)$$

G_M: a constant (to be defined below)

$$\phi_M^{**} = [(1 + \phi''_M)/(1 + {}^1k_{21}\,{}^1k'^{-1}_M)] - 1 \qquad (26)$$

$$\phi''_M = {}^1k_{12}[H^+][^1R]_M I_a^{-1} \qquad (27)$$

$${}^1k'_M = k_{F(RH)} + k_{C(RH)} + {}^1k_{Q(RH)}[Q] + k_{STM(RH)} \qquad (28)$$

$$U_M = ({}^3k_M[^3R] + {}^3k'[^3RH])/k'_{32} + k_{34} \qquad (29)$$

and:

$${}^3k_M = k_{PM(R)} + {}^3k_Q[Q] + k_{TSM(R)} \qquad (30)$$

If there is any enhancement of the BZA's $S_1 \rightsquigarrow T_1$ crossing, the ratio (compare (22) with (1)):

$$\frac{(\overleftarrow{k}_{irM} - \overleftarrow{k}_{GM})(1 + \beta[M^{n+}])G}{(\overleftarrow{k}_{ir} - \overleftarrow{k}_G)G_M} = \frac{\Phi_{STM}}{\Phi_{ST}} \qquad (31)$$

(where $\overleftarrow{k}_{ir}$, $\overleftarrow{k}_G$, G refer to "B–BZA" complexation in the absence of M^{n+}), must be higher than unity.

Table I shows that this is indeed the case for all the metal ions used in this work and it can therefore be concluded that these ions enhance $S_1 \rightsquigarrow T_1$ crossings of the photoactive R form of BZA.

TABLE I. Triplet Quantum Yield Ratio (Φ_{STM}/Φ_{ST}) of BZA in the Presence of Heavy-metal Ion.[a]

M^{n+}	$\overleftarrow{k}_{irM}$	$\overleftarrow{k}_{GM}$	β_M	G/G_M	Φ_{STM}/Φ_{ST}
Ag^+	0.0636	0.0541	600	1.03	1.79
Cd^{2+}	0.0737	0.0645	9500	1.04	1.81
Hg^{2+}	0.068	0.0562	10000	1.04	2.33
Tl^+	0.0643	0.0557	1800	1.05	1.84

[a] $\overleftarrow{k}_{ir} = 0.062$, $\overleftarrow{k}_G = 0.0562$ and $G = 1.94$ [2] for "B–BZA" chelate formation in the absence of M^{n+}.

*Any influence of HMI to the $S \longleftrightarrow T$ crossings of the protonated form RH of BZA can be disregarded, since CT states intervening in external perturbations are improbable.

G_M was calculated by (see (2)):

$$G_M = \frac{1 - e^{-2.3031([1+(q-1)\gamma+\delta]\epsilon_R[R]_0+(\epsilon_{AR}-\epsilon_R)[AR])}}{(1+(q-1)\gamma+\delta)\epsilon_R[R]_0+(\epsilon_{AR}-\epsilon_R)[AR]} \simeq$$

$$\simeq 2.303 - 2.652(1+\delta)\epsilon_R[R]_0$$

where

$$\delta = \epsilon_{MR}[(RM)^{n+}]/\epsilon_R[R]_0 \simeq [(RM)^{n+}]/[R]_0 =$$

$$\frac{-[R]_0[M^{n+}] + \beta_M^{-1} \pm [([R]_0[M^{n+}] + \beta_M^{-1})^2 + 4[R]_0[M^{n+}]_0]^{1/2}}{2[R]_0}$$

Starting from the relation (23), we can now examine the lowering of $\vec{k}_{GM}$ (forward chelate formation rate constant in the presence of HMI) upon ligand excitation (compare D with C in Figs. 1 to 4).

Combining (23) with (26), we find:

$$Q_M = \frac{\vec{k}_{irM}^{-1} - \vec{k}_{GM}^{-1}}{\vec{k}_{GM}^{-1} G_M}$$

$$= \left[1 - \frac{(1+\phi_M'')}{(1+{}^1k_{21}{}^1k_M'^{-1})}\right] k_{21}^{-1} \epsilon_{RH} V^{-1} I_0'$$

$$= \left[\frac{{}^1k_{21}{}^1k_M'^{-1} - \phi_M''}{1+{}^1k_{21}{}^1k_M'^{-1}}\right] k_{21}^{-1} \epsilon_{RH} V^{-1} I_0' \qquad (32)$$

and since one can reasonably expect that ${}^1k_M'$ of the protonated form of BZA is very little or at all affected by HMI (*i.e.* ${}^1k_M' = {}^1k'$), Q_M must be higher than Q (in the absence of HMI), since, owing to a more active BZA $S_1 \rightsquigarrow T_1$ crossing in the presence of HMI, $[{}^1R]_M$ (see (27)) must be lower than $[{}^1R]$.

The values of Q and Q_M in Table II are, indeed, in agreement with the above "excited-state-process" expectations, so that the variations in both $\vec{k}_{GM}$ and $\vec{k}_{GM}$ under continuous ligand excitation clearly suggest a $S_1 \rightsquigarrow T_1$ enhancement of BZA, which influences the rate of the ^{3}(borobenzoylacetonide) [1, 2] excited-state complex formation.

TABLE II. Q Values for unperturbed BZA and in the Presence of Metal Ions.

M^{n+}	O	Ag^+	Cd^{2+}	Hg^{2+}	Tl^+
$\vec{k}_G$	17.9	16.9	16.4	16.3	15.2
$\vec{k}_{ir}$	15.2	14.0	8.1	10.4	11.0
Q	0.092	0.11	0.548	0.303	0.207

Finally, we may discuss the U functions, which (see (3a) and (29)) are informative of the $T_1 \rightsquigarrow S_0$ processes of BZA.

TABLE III. U Values for Unperturbed and Perturbed BZA.

$[A]_0 = 1.5 \times 10^{-3}$ [a]					
M^{n+}	O	Ag^+	Cd^{2+}	Hg^{2+}	Tl^+
$U \times 10^7$	1.1	1.3	0.4	1.0	0.9
$[A]_0 = 3.2 \times 10^{-3}$					
$U \times 10^7$	2.1	2.1	0.5	1.5	1.4

[a] $[A]_0$ = total boric acid concentration.

As shown in Table III, the U values obtained from (3) and (29) are insensitive to the HMI.

This may be explained, on the basis of the mechanism below [2], as follows:

$$R \xleftarrow{{}^3k \text{ or } {}^3k_M} {}^3R \rightleftharpoons {}^3RH \xrightarrow{{}^3k'} {}^3RH$$

${}^3k_M[{}^3R]$ in expression (29) is undoubtedly higher than the first kinetic term in (3a), since as was found, $k_{STM} > k_{ST}$ and τ_R diminishes (Fig. 12) in the presence of HMI. The more active degradation of ^3R by the HMI results, however, in a higher competition of the $^3R \rightarrow {}^3RH$ protolytic path, so that the increase in ${}^3k_M[{}^3R]$ relative to ${}^3k[{}^3R]$ results in a simultaneous decrease of ${}^3k'[{}^3RH]$, making U insensitive to the HMI perturbation.

Acknowledgments

I am grateful to Mrs. Y. Zakaria, who carried out most of the experimental work.

References

1 M. Marcantonatos, *Inorg. Chim. Acta, 19,* 109 (1976).
2 M. Marcantonatos, *Inorg. Chim. Acta, 16,* 17 (1976).
3 O. L. J. Gijzeman, F. Kaufman and G. Porter, *J. Chem. Soc. Faraday II, 69,* 708 (1973); *69,* 727 (1973).
4 O. L. J. Gijzeman and F. Kaufman, *J. Chem. Soc. Faraday II, 69,* 721 (1973).
5 O. L. J. Gijzeman, *J. Chem. Soc. Faraday II, 70,* 1143 (1974).
6 H. Leonhardt and A. Weller, *Z. Elektrochem., 67,* 791 (1963); *Z. Phys. Chem. (N.F.), 29,* 277 (1961).
7 D. G. Whitten, J. W. Happ, G. L. B. Carlson and M. T. McCall, *J. Am. Chem. Soc., 92,* 3499 (1970).
8 R. F. Steiner and E. P. Kirby, *J. Phys. Chem., 73,* 4130 (1969).
9 K. Vashihara, K. Futamura and S. Nagakura,, *Chem. Letters,* 1243 (1972).
10 G. Porter and M. R. Wright, *Disc. Faraday Soc., 27,* 18 (1959).
11 H. Linschitz and L. J. Pekkarinen, *J. Am. Chem. Soc., 82,* 2411 (1960).
12 M. Zander, *Z. Naturforsch., 26a,* 1371 (1971).
13 R. H. Hofeldt, R. Sahai and S. H. Lin, *J. Chem. Phys., 53,* 4512 (1970).
14 V. Breuninger and A. Weller, *Chem. Phys. Letters, 23,* 40 (1973).
15 J. Zechner, G. Köhler, G. Grabner and N. Getoff, *Chem. Phys. Letters, 37,* 297 (1976).

16 J. Nag-Chaudhuri and S. Basu, *Trans. Faraday Soc., 54,* 1605 (1958).
17 F. J. Wright, *J. Phys. Chem., 65,* 381 (1961).
18 J. Nag-Chaudhuri, L. Stoessell and S. P. McGlynn, *J. Chem. Phys., 38,* 2027 (1963).
19 C. Steel and H. Linschitz, *J. Phys. Chem., 66,* 2577 (1962).
20 A. Adamczyk and F. Wilkinson, *J. Chem. Soc. Faraday II, 68,* 2031 (1972).
21 A. Farmilo and F. Wilkinson, *Chem. Phys. Letters, 34,* 575 (1975).
22 A. Vander Donckt, D. Liétar and M. Matagne, *J. Chem. Soc. Faraday II, 69,* 322 (1973).
23 J. C. Scaiano, *J. Photochem., 2,* 315 (1974).
24 D. F. Evans, *J. Chem. Soc.,* 3885 (1957).
25 N. Christodouleas and S. P. McGlynn, *J. Chem. Phys., 47,* 2203 (1967).
26 S. P. McGlynn, T. Azumi and M. Kinoshita, "Molecular Spectroscopy of the Triplet State", Prentice-Hall, London, p. 321–5 (1969).
27 M. Marcantonatos and G. Gamba, *Helv. Chim. Acta, 52,* 2183 (1969).
28 R. S. Mulliken and W. B. Person, "Molecular Complexes", Wiley–Interscience, New York, p. 154 (1969).
29 J. B. Birks, "Photophysics of Aromatic Molecules", Wiley–Interscience, London, p. 415 (1970).
30 N. Mataga and Y. Murata, *J. Am. Chem. Soc., 91,* 3144 (1969).
31 H. B. Gray, "Les électrons et la liaison chimique", Ediscience, Paris (1969) p. 164.
32 F. Herman and S. Skillman, "Aromatic Structure Calculations", Prentice–Hall, London (1963).
33 "Stability Constants", Supplement No. 1, The Chemical Society, London, p. 398 (1971).